Lipin1 Alleviates Autophagy Disorder in Sciatic Nerve and Improves Diabetic Peripheral Neuropathy

Meijian Wang
Shandong University https://orcid.org/0000-0003-1021-2421
Min Xie
Shandong University
Shuyan Yu
School of Basic Medical Sciences, Shandong University
Pan Shang
Shandong University
Cong Zhang
Qingdao Technical College
Xiaolin Han
Shandong University
Cuiqin Fan
School of Basic Medical Sciences, Shandong University
Li Chen
Shandong University
Xianghua Zhuang
Shandong University
Shihong Chen (chenshihong26@163.com)
Shandong University

Research Article

Keywords: Lipin1, Diabetic peripheral neuropathy, Autophagy, Sciatic nerve, RCS96 cell.

Posted Date: May 11th, 2021

DOI: https://doi.org/10.21203/rs.3.rs-437178/v1

Version of Record: A version of this preprint was published at Molecular Neurobiology on August 26th, 2021. See the published version at https://doi.org/10.1007/s12035-021-02540-5.

Abstract

Diabetic peripheral neuropathy (DPN) is a chronic complication of diabetes, and its exact pathogenesis remains unclear. Autophagy plays an important role in neurodegenerative diseases, ischemia–reperfusion injury of nerve tissues, and nerve tissue injury repair. Lipin1 is a phosphatidic acid phosphatase enzyme that converts phosphatidic acid (PA) into diacylglycerol (DAG), a precursor of triacylglycerol and phospholipids which plays an important role in maintaining normal peripheral nerve conduction function. Here, we show that induction of DPN rat model via STZ injection could reduce Lipin1 expression, prevent DAG synthesis, and results in autophagic hyperactivity. Interestingly, these effects increase the apoptosis of Schwann cells and lead to demyelination in sciatic nerve in DPN rats. More importantly, upregulation of lipin1 in the DPN rats ameliorated autophagy disorders and pathological changes of the sciatic nerve, which associated with the increase of the motor nerve conductive velocity (MNCV) in DPN rats. In contrast, lipin1 downregulation exacerbates neuronal abnormalities and facilitates the genesis of DPN phenotypes in rats. In addition, overexpression of lipin1 in RSC96 cells also significantly decreased the autophagic hyperactivity and apoptosis induced by hyperglycemia. These results suggest that lipin1 may exert neuroprotection within the sciatic nerve anomalies and may serve as a potential therapeutic target for the treatment of DPN.

1. Introduction

With the development of economy and the progress of society, the incidence of diabetes is increasing worldwide [1, 2]. The incidence of chronic complications of diabetes increases with prolonged human life and improved medical conditions [3, 4]. Diabetic peripheral neuropathy (DPN) is a chronic complication of diabetes that is knotty and ineffective [5]. Patients may have spontaneous pain, hyperalgesia, acupuncture-like pain, and other symptoms, which may lead to diabetic foot ulcer, gangrene, or amputation. This condition severely affects the quality of life of patients [6, 7]. At present, the exact pathogenesis of DPN remains unclear [8, 9]. No specific etiology treatment has been established and must be solved in the medical field.

Autophagy plays an important role in neurodegenerative diseases, ischemia–reperfusion injury of nerve tissues, and repair of nerve tissue injury. In patients with DPN, autophagy disorder occurs in nerve tissues due to long-term hypoxia, lack of nerve factors, and oxidative stress [10]. In 1966, Duve first expounded autophagic vesicles/lysosomes. The number of autophagy/autophagy lysosomes in neurons increases under various conditions, such as axonal injury, toxic exposure, and genetic degenerative disease model [11, 12]. Wang et al. confirmed that autophagy is induced in mouse Purkinje cells during axonal atrophy and degeneration; hence, autophagy dysfunction may be one of the potential mechanisms of axonal diseases [13]. However, the relationship between autophagy and peripheral nerve injury, especially in diabetic peripheral neuropathy, has been rarely studied.

Lipin1 is an enzyme closely related to glycolipid metabolism produced by the expression of LIPIN [14]. Lipin1 plays an important role in maintaining normal peripheral nerve conduction function [15]. In our

previous study, we found that cognitive impairments were present in Lpin1^{fld}/J mice via DAG-PKD-ERK pathway [16]. Furthermore, the expression of lipin1 in the hippocampal CA1 region was also decreased, while upregulation of lipin1 expression could improve diabetic encephalopathy in rats [17]. However, whether Lipin1 influences peripheral nerve function in DPN by regulating autophagy remains unclear. Therefore, in the present study, we constructed DPN rat models and explored the mechanism of Lipin1 in the pathogenesis of diabetic autophagy disorder.

2. Materials And Methods

2.1. Animals

Adult male Wistar rats, weighing 150–185g (or 5-6 weeks-old), obtained from the Experimental Animal Center of Shandong University, were used throughout the study. All rats were housed in a temperature and humidity-controlled environment under a 12 h light/dark cycle with free access to water and a standard rodent chow diet. In the handling and care of all animals, the International Guiding Principles for Animal Research as stipulated by the World Health Organization were followed.

2.2. Cells

RSC96 cells (CRL-2765) were obtained from the American Type Culture Collection (ATCC, cat no. CRL-2765) and were cultured in DMEM modified to contain 4 mM L-glutamine, 25 mM glucose, 1 mM sodium pyruvate, 1500 mg/L sodium bicarbonate, 10% FBS, 100 IU penicillin and 100μg/ml streptomycin at 37 °C in a humidified atmosphere of 5% CO2 and were passaged once every 3-4 days.

2.3. Virus packaging

Lipin1 overexpression and low expression of adenovirus and lentivirus were purchased from GeneChem, Shanghai, China. Adenovirus and lentivirus were carried eGFP. The Lipin1 overexpression and low expression of adenovirus (ADV-Lipin1/ ADV-Lipin1-RNAi) and corresponding adenovirus empty shell control (ADV-Lipin1-Con/ADV-Lipin1-RNAi-Con) were separately packaged. We also packaged Lipin1 overexpression and low expression of lentivirus (LV-Lipin1/ LV-Lipin1-RNAi), as well as the corresponding lentivirus empty shell control (LV-Lipin1-Con/LV-Lipin1-RNAi-Con). The titers of ADV-Lipin1, ADV-Lipin1-RNAi, ADV-Lipin1-Con, and ADV-Lipin1-RNAi-Con were 4.0×10^{10}PFU/ml, 1.5×10^{10}PFU/ml, 5.0×10^{10}PFU/ml and 1.0×10^{10}PFU/ml separately. The titers of LV-Lipin1, LV-Lipin1-RNAi, LV-Lipin1-Con, and LV-Lipin1-RNAi-Con were 1.0×10^{9}TU/ml, 7×10^{8}TU/ml, 2.0×10^{9}TU/ml and 1.0×10^{9}T U/ml separately. The transfection and expression efficiency of both high and low expression viruses were up to standard. The sequence of Lipin1-RNAi was caGCGAGTCTTCAGACACTTT. The sequence of Lipin1-RNAi-Con is TTCTCCGAACGTGTCACGT.

2.4. Animal model of DPN and virus intrathecal injection

Rats were first divided into negative control (NC) and diabetes mellitus (DM) group. All rats were adaptive feeding for one week in the rat room. After one week, DM was induced by intraperitoneal injection of streptozotocin (STZ, 55 mg/kg in 0.1 M citric acid buffer, pH 4.5). The rats with a fasting blood glucose levels above 16.7 mM 3-day after STZ injection were considered diabetic and were continued feeding for 8 weeks. Fasting blood glucose levels were measured 3-day, 1-week, 2-week, 4-week, 6-week, and 8-week after STZ injection to monitor the persistence of diabetes and paw mechanical withdrawal threshold (PMWT) were measured every 4 weeks to track the occurrence of peripheral neuropathy.

After the DPN rats were modeled, that is, 8 weeks after the diabetic rats were modeled, DM rats were divided into two groups, Lipin1 overexpression group (ADV-Lipin1) and Adenovirus empty shell group (ADV-Lipin1-Con). Meanwhile, NC rats were also divided into two groups, Lipin1 low expression group (ADV-Lipin1-RNAi) and Adenovirus empty shell group (ADV-Lipin1-RNAi-Con). And then intrathecal injection of ADV was carried out. Rats were anesthetized with sodium pentobarbital (40mg/kg) and removed the hair from the lumbar part of the rats to expose the skin, and 75% alcohol was used for disinfection. The rats were punctured into the subarachnoid space between the lumbar 3-4 or lumbar 4-5 with a special 25ul micro syringe(Feige, Nanjing, China) [18,19]. The tail flick reflex of the rats was used as a sign of the micro syringe entering the sheath. Then slowly injected four different ADV viruses, 20ul per rat, the injection time lasted no less than 5 minutes, stayed for 2 minutes, and then slowly pulled out the micro-injection needle. Disinfect the skin again, the rats were awakened in the incubator and moved into the ordinary feeding box. After 2 weeks of intrathecal injection, behavioral tests were performed, and rats were killed and sciatic nerves were taken.

2.5. Cell transfection

Cell culture and transfection. RSC96 cells plated at a density of 5.0×10^4cells/well in 6-well plates were allowed to adhere overnight and then transfected with four kinds of lentivirus according to the manufacturer's instructions. According to the MOI value of RSC96 cells, the corresponding virus amount was added (Virus volume = (MOI×cell number) / virus titer). RSC 96 cells were incubated 12-16 hours at 37 °C in a CO_2 incubator, 2ml conventional medium was added to replace the infection mixture. Cells were incubated for an additional 72 hours and the medium can be changed every 2 days to keep cell activity. 72 hours after infection, the following test was continued. Cells were aspirated and cultured in 25 mM or 100 mM glucose growth medium for 48 hours, respectively. Lipin1 low expression LV (LV-Lipin1-RNAi) and empty shell control (LV-Lipin1-RNAi-Con) group were treated with 25mM glucose, while Lipin1 overexpression LV (LV-Lipin1) and empty shell control (LV-Lipin1-Con) group were treated with 100mM glucose.

2.6. Measurement of paw mechanical withdrawal threshold (PMWT)

In a quiet environment, the rats were placed in a transparent plexiglass cover with a mesh pad made of metal wire at the bottom. After the rats adapted to the environment for 15 minutes until they were in a quiet state, the rats' PMWT was measured with the acupuncture pain test kit (vonfrey, Aesthesio, danmic

Global, USA, measuring range of 0.008g-300g stimulation) [20]. The skin between the third and fourth toes of the rats was pressed vertically with nylon wires using different stimulating forces (the nylon wires were bent each time). When the rats had rapid retraction, hind foot lifting, quick swing, licking, and hissing after shaking their feet, the pressure was stopped, and the stimulation force was taken as the PMWT. Each rat was repeated 3 times. Each measurement included the left and right feet, each interval of 5 minutes. The average value of each measurement was taken as the PMWT.

2.7. Measurement motor nerve conduction velocity (MNCV) of sciatic nerve

Nerve conduction velocity was assessed using Functional Experiment System (BL-420s, Techman, China) as reported previously. Rats were anesthetized with isoflurane, then the left lower leg hair was removed, the skin was exposed. The skin of the sciatic node and the passing part of the sciatic nerve of the ankle joint were cut, and the sciatic nerve was carefully separated [21]. The stimulation electrode (S1) is located at the ischial notch, and the recording electrode (S2) is located at the ischial nerve passing through the ipsilateral ankle joint. The reference electrode (E) is located between S1 and S2, 1cm away from S2. Sciatic nerve was stimulated with single square wave pulses (1.2V in intensity, 1ms in width), and a biphasic compound action potential was recorded from S2. Repeat the measurement 5 times. MNCV (m/s) = sciatic nerve length (between S1 and S2) / nerve conduction time.

2.8. Electron microscopy (EM)

Electron microscopy (EM) analysis was performed to assess sciatic nerve and RSC96 cell ultrastructure. The tissues or cell sedimentation were then placed in 2.5% glutaraldehyde at 4 ◦ C for 24 h, followed by fixation with 1% osmium tetroxide for 2 h. After a series of graded ethanol dehydrations, the tissues or cell sedimentation were infiltrated with a mixture of one-half propylene oxide overnight and embedded in resin. The tissues or cell sedimentation were then cut into ultrathin sections (70 nm) and stained with 4% uranyl acetate for 20 min followed by 0.5% lead citrate for 5 min. Sciatic nerve and RSC96 cell ultrastructure were observed using EM (Philips Tecnai 20 U-Twin, Holland).

2.9. Quantitative real-time PCR (qPCR)

Total RNA was isolated and extracted from sciatic nerve and RSC96 cell samples using the Trizol Reagent (Invitrogen, USA). Total RNA (1μg) was reverse-transcribed into cDNA by using the PrimeScript^{TM} RT reagent Kit with a gDNA Eraser (TaKaRa, Japan) according to the manufacturer's instructions. The reverse transcription reaction was amplified using a Bio-Rad CFX96 Detection System (Bio-Rad, USA). Quantitative Real time PCR was performed with use of the ChamQ SYBR qPCR Master Mix (TaKaRa, Japan) on the Bio-rad IQ5 Real Time PCR System (Bio-Rad, USA). Reaction conditions were: 95◦C for 2 min and 40 cycles of the amplification step (denaturation at 95◦C for 5 s, annealing at 55◦C for 5 s, and extension at 72◦C for 25 s). The following primers were used for qPCR: Lipin1-forward TATGACACGGCTTGTTCC; reverse GTGGCTGCCCTGTATTTC; β-actin-forward CCTAGACTTCGAGCAAGAGA; reverse GGAAGGAAGGCTGGAAGA; β-Actin served as a loading control in each sample, and targeted gene expression levels were evaluated using the $2^{-\Delta\Delta Ct}$ method [22].

2.10. Western Blot

Sciatic nerves and RSC96 cells were lysed on ice in RIPA buffer with protease inhibitor cocktail and phosphatase inhibitor cocktail for 30 min and centrifuged at 1000 × g for 15min at 4◦C to extract total protein. The proteins were analyzed with a bicinchoninic acid (BCA) protein assay kit (Pierce Biotechnology, Inc., US). Equal amounts of protein (30μg) were subjected to SDS-PAGE analysis. The resolved proteins were transferred to PVDF membranes (Millipore, Bedford, MA). PVDF membranes were blocked in 5% nonfat milk for 1 h and then incubated overnight at 4 °C with the appropriate primary antibodies. The primary antibodies were as follows: rabbit anti-Lipin1 (1:250, Cell Signaling Technology, Beverly, MA), rabbit anti-P62 (1:500, Cell Signaling Technology, Beverly, MA), rabbit anti-LC3B (1:500, Cell Signaling Technology, Beverly, MA), rabbit anti-β-actin (1:5000, Cell Signaling Technology, Beverly, MA).After washing in TBS-T, blots were exposed to the appropriate secondary antibodies (1:5000, Abcam Co., UK) in TBS-T for 1 h at room temperature. Western Chemiluminescent HRP Substrate (Millipore Corporation, Billerica, MA01821, US) was used to form image. Blots were developed using ChemiDocTM Imager from Bio-Rad. The protein bands were quantitated with Image J software and normalized to β-actin.

2.11. Measurement of diacylglycerol (DAG)

An enzyme-linked immunosorbent assay (ELISA) kit (IL20977-96T, Shanghai Jianglai industrial Limited by Share Ltd, China) was used to measure rat diacylglycerol (DAG) according to the manufacturer's instructions. The sciatic nerves were rinsed by precooling PBS to remove the residual blood. After weighing, the tissues were cut into pieces. The cut tissues and PBS of the corresponding volume (1mg: 9ul) were added into the glass homogenizer and fully ground on ice. If necessary, ultrasonic breaking or repeated freezing and thawing were carried out. Centrifugation at 5000rpm for 5min, and take the supernatant for test.

2.12. Apoptosis assay

An Annexin-FITC Apoptosis Detection Kit (556547, BD Biosciences, USA) was used to examine apoptosis according to the manufacturer's instructions. In brief, cells were added with 300μL of binding buffer followed by staining with 5μL of FITC-labeled annexin V and 5μL of propidium iodide (PI) and incubated at room temperature for 20 min in the dark. After lentivirus transfected RSC96 cells, an Annexin-APC Apoptosis Detection Kit (E-CK-A218, Elabscience, China) was used to examine apoptosis according to the manufacturer's instructions. Cells were added to 300μL of binding buffer followed by staining with 5μL of APC-labeled annexin V and 5μL of 7-Aminoactinomycin (7-AAD) and incubated at room temperature for 20 min in the dark.BD LSRFortessa™ flow cytometer (BD Biosciences, San Jose, CA, USA) were used for analysis.

2.13. Cell Counting Kit-8 (CCK8)

An Cell Counting Kit-8 (CK04-500T, Dojindo, Japan) was used to examine the activity according to the manufacturer's instructions. RSC96 cell suspension (100ul/well, about 3000-5000 cells/well) was inoculated in 96- well plate and cultured in an incubator for 48 hours (37 ℃, 5% CO2). Add a 10ul CCK-8 solution to each hole (be careful not to generate bubbles in the hole, they will affect the reading of O.D value). Incubate the plates in the incubator for 2-4 hours. The absorbance at 450 nm was determined by enzyme scale.

2.14. Statistical analysis

Data were expressed as means ± SEM. Statistical analysis was performed by two-tailed Student's t-test or one-way ANOVA using SPSS 17.0. A p value < 0.05 was considered statistically significant.

3. Results

3.1. Lipin1 expression is decreased in DPN rats.

In this study, we intraperitoneally injected STZ (55 mg/kg) to induce DPN in the rat model, and we found that from the third day after STZ injection, body weights were significantly decreased (P <0.01), and fasting blood glucose (FBG) levels significantly increased (P <0.01) in the DPN group as compared with that of the negative control (NC) group (Fig.1A). The motor nerve conductive velocity (MNCV) of the sciatic nerve and paw mechanical withdrawal threshold (PMWT) of DPN rats decreased compared with that of NC group (P <0.01, respectively) (Fig.1B, C). Sciatic nerve showed degenerative and demyelinating changes in DPN rats. The demyelination of the sciatic nerve occurred. The lamella was loose and broken (Fig.1F). The levels of diacylglycerol (DAG) decreased in the sciatic nerve in DPN group as compared with that of NC group (P <0.01, Fig.1E). Furthermore, the mRNA (P <0.05, Fig.1D) and protein (P <0.01, Fig.1G) expression levels of Lipin1 in the sciatic nerve of DPN group were all significantly decreased than that of NC group, consistent with our previous study [23]. In addition, the expression of the autophagy-related protein P62 decreased (P <0.01) in the sciatic nerve of DPN rats as compared with that in NC group (Fig.1G), whereas the LC3II expression level increased (P <0.01) in the sciatic nerve of DPN group than NC group(Fig.1G).

3.2. Overexpression of Lipin1in DPN rats ameliorated autophagy disorders and pathological changes.

The Lipin1 expression decreased, and autophagy increased in the sciatic nerve of DPN rats. Whether increasing Lipin1 expression can improve behavior and autophagy disorders in the sciatic nerve remains unknown. To verify the role of Lipin1 in the sciatic nerves of DPN rats, we intrathecally injected ADV-Lipin1 to construct a Lipin1 high-expression DPN rat model (Fig.2A). After intrathecally injected of different ADV viruses, the mRNA (P <0.05, Fig.2D) and protein (P <0.05, Fig.3E) expression levels of Lipin1 in the sciatic nerve of ADV-Lipin1 group were all significantly increased than that of ADV-Lipin1-Con group. After the overexpression of lipin1, PMWT and MNCV in ADV-Lipin1 rats were slightly improved than those in ADV-Lipin1-Con group (Fig.2B, C). After overexpression of Lipin1, the structure of myelin sheath of sciatic nerve fibers and the myelin sheath separation improved significantly and the lamella

was dense (Fig.3A). After the overexpression of lipin1, DAG (P <0.01, Fig.3B) significantly increased and P62 (Fig.3D,E) slightly increased, while LC3II (P <0.05, Fig.3D,E) decreased.

3.3. Downregulation of Lipin1 in normal rats induced phenotypes of DPN.

To explore the role of Lipin1 in the sciatic nerves of normal rats, we intrathecally injected the small interference RNA sequence form of lipin1 in the ADV virus (ADV-Lipin-1-RNAi) to reduce the expression of Lipin1 in the sciatic nerve of normal rats and observed the changes in the behavior and sciatic nerves in rats. After virus intrathecally injected, the mRNA (P <0.01, Fig.2D) and protein (Fig.3C, E) expression levels of Lipin1 in the sciatic nerve of ADV-Lipin1-RNAi group were all decreased than that of ADV-Lipin1-RNAi-Con group. In ADV-Lipin1-RNAi rats, PMWT and MNCV were decreased than that in ADV-Lipin1-RNAi-Con rats (Fig.2B, C). Meanwhile, the sciatic nerve showed mild swelling in ADV-Lipin1-RNAi rats and the lamella was loose compared with ADV-Lipin1-RNAi-Con rats (Fig.3A). The DAG levels (P <0.01, Fig.3B) of sciatic nerve significantly decreased in ADV-Lipin1-RNAi rats than that in ADV-Lipin1-RNAi-Con rats. After the low expression of lipin1, P62 (P <0.05) decreased, while LC3II (P <0.01) significantly increased (Fig.3D, E).

3.4. Hyperglycemia reduced the expression of Lipin1 in RSC96 cells.

To further verify the role and underlying mechanisms of Lipin1 in DPN, we cultured Schwann cells (RSC96 cells) in vitro with normal glucose (25Mm/48h) and high glucose (100Mm/48h) to imitate DPN. We found that cell activity decreased (P <0.05, Fig.4B) in 100mM than 25mM. Meanwhile, cell apoptosis increased (P <0.05, Fig.4D) in 100mM higher than 25mM. Based on observations using an electron microscope, the number of autophagic bodies in RSC96 cells were increased in 100mM more than 25mM (Fig.4A). The mRNA (P <0.01, Fig.4E) and protein (P <0.01, Fig.4F) expression levels of Lipin1 were significantly decreased in 100mM than 25mM. The levels of DAG also decreased in 100mM more than 25mM (P <0.01, Fig.4C). We also found that the P62 decreased (P <0.01) in 100mM more than 25mM, whereas the LC3II expression level increased (P <0.01) in 100mM more than 25mM (Fig.4G).

3.5. Overexpression of Lipin1 in RSC96 cells ameliorated the injury induced by hyperglycemia

Hyperglycemia can reduce Lipin1 expression, decrease cell activity, and increase apoptosis in RSC96 cells. Whether increasing the expression of Lipin1 can alleviate these changes remains unknown. We transfected RSC96 cells with LV-Lipin1 overexpressing virus to enhance the expression of Lipin1 (Fig.5A). The mRNA (P <0.01, Fig.5E) and protein (P <0.01, Fig.5F, G) expression levels of Lipin1 in RSC96 cells of LV-Lipin1 group were significantly increased than that of LV-Lipin1-Con group. Cell activity increased in LV-Lipin1 group than LV-Lipin1-Con group (P <0.01, Fig.5B), while cell apoptosis slightly decreased in LV-Lipin1 group than LV-Lipin1-Con group (Fig.5D). In LV-Lipin1 group, autophagy bodies decreased in the cytoplasm in RSC96 cells (Fig.5A). Besides, P62 slightly increased and the LC3II expression level decreased in LV-Lipin1 group than LV-Lipin1-Con group (Fig.5F, G).

3.6. Downregulation of Lipin1 induced injury of RSC96 cells.

Whether RSC96 cells show similar changes in normal glucose (25Mm/48h) after decreasing the expression of Lipin1 remains unclear. We then transfected RSC96 cells with LV-Lipin1-RNAi low expression virus to reduce the expression of Lipin1 (Fig.5A) in normal glucose. We found the mRNA ($P < 0.01$, Fig.5E) and protein ($P < 0.01$, Fig.5F,G) expression levels of Lipin1 in RSC96 cells of LV-Lipin1-RNAi group were significantly decreased than that of LV-Lipin1-RNAi-Con group. In LV-Lipin1-RNAi group, autophagy bodies increased in the cytoplasm in RSC96 cells (Fig.5A). Cell activity decreased in LV-Lipin1-RNAi group than LV-Lipin1-RNAi-Con group ($P < 0.01$, Fig.5B), while cell apoptosis slightly increased in LV-Lipin1-RNAi group than LV-Lipin1-RNAi-Con group ($P < 0.01$, Fig.5D). Moreover, P62 significantly decreased and the LC3II expression level significantly increased in LV-Lipin1-RNAi group than LV-Lipin1-RNAi-Con group ($P < 0.05$, respectively, Fig.5F, G).

4. Discussion

DPN is a degenerative disease, which may be related to oxidative stress, glycosylation end products, polyol pathway, lack of neurotrophic factors, and microcirculation disorders [24–28]. Typical changes in neuropathology include axonal injury, focal segmental deletion of myelin, and neuronal damage [29]. Hyperglycemia, advanced glycation end products, polyols, oxidative stress, and other stimuli act as noxious stimulus signals, which can damage sensory neurons and axons. In normal nerves, Schwann cells surround axons to form the myelin sheath and nutrition nerves. However, under the harmful stimulation of hyperglycemia, Schwann cells proliferate and migrate again, resulting in axonal degeneration and demyelination.

Autophagy is common in eukaryotic cells and plays a crucial role in maintaining cell homeostasis and body function [30]. Autophagy is the major pathway to clear large targets for degradation, such as protein aggregates and dysfunctional organelles. Neurons are postmitotic and cells with long life. Neurodevelopment and neuronal health require effective removal of aggregated proteins and aged or defective organelles. Normal autophagy is essential for the survival, differentiation, growth, and maintenance of homeostasis of the body, which can cope with the adverse environment. Neurodegeneration is one of the many different afflictions that autophagy impairment can cause to human [31].

Lipin1 is a phosphatidic acid phosphatase (PAP) enzyme that converts phosphatidic acid (PA) to DAG, which is a precursor of triacylglycerol and phospholipids [32, 33]. The PAP activity of Lipin1 is required for the generation of DAG and activation of the PKD signaling pathway in autophagy clearance. Lipin1 deficiency reduces DAG levels and impairs the activation of PKD–Vps34, preventing the maturation of autolysosomes and destroying autophagy homeostasis [34]. In previous studies, autophagy in the sciatic nerve of diabetic rats is weakened [35]; other studies reported enhanced autophagy [13]. In Lipin1-deficient mice, a disorder of peripheral nerve myelination, including demyelination and axonal degeneration, has been observed [15]. In our research, we found that hyperglycemia reduced Lipin1 expression in the sciatic nerve of rats, as well as reduced DAG levels. MNCV of DPN rats are lower than

that in NC rats. Morphological changes in the sciatic nerve are observed in DPN rats, such as demyelination and degenerative (Fig. 1F).

RSC96 cells, rat Schwann cells, has been widely used in neurophysiological studies in vitro [36–38]. Schwann cell dysfunction directly affects neuronal function due to myelin disruption and demyelination [30]. Schwann cells are the glial cells responsible for producing the myelin sheath in the PNS and are highly susceptible to autophagy. Therefore, high glucose-treated Schwann cells were used for investigation. In vitro experiments, hyperglycemia reduces Schwann cell activity and increases apoptosis rate and increases the number of autophagic bodies.

LC3 and P62 are the main proteins regulating cell autophagy [39]. When autophagy is formed, cytoplasmic LC3 will hydrolyze a small segment of polypeptide to form LC3I, and then LC3I will be transformed into LC3-II. While autophagy increased, LC3II increased and P62 decreased [40]. In our study, we observed that autophagy were increased in the sciatic nerves of diabetic rats and high glucose–treated RSC96 cells compared with the normal control group. Hyperglycemia enhances autophagy in vivo and in vitro because of increased LC3II and decreased P62. Hyperglycemia decreases the level of Lipin1, obstructs PA synthesis DAG, and enhances autophagy. Excessive enhancement of autophagy impairs the sciatic nerve and damages Schwann cells.

After the overexpression of Lipin1 in the sciatic nerve of DPN rats through the intrathecal injection of ADV-Lipin1, we observed that the sciatic nerve morphology of DPN rats (Fig. 3A) and MNCV (Fig. 2C) ameliorated. Decreased LC3II and increased P62 indicate that autophagy has been decreased and autophagy disorder has been reduced. In vitro experiments showed that Schwann cells transfected with LV-Lipin1 increases cell activity, decreases apoptosis rate, improves cell morphology, and decreases autophagy.

When we used ADV-Lipin1-RNAi to reduce the expression of Lipin1 in the sciatic nerve of NC rats, we were surprised to find that the sciatic nerve of NC rats had similar changes to DPN rats (Fig. 3A). MNCV is slightly lower than that in NC rats. Autophagy is slightly enhanced in ADV-Lipin1-RNAi group than NC rats. When we transfected Schwann cells with LV-Lipin1-RNAi virus under normal glucose concentration, they showed similar changes as well as in high glucose environment.

Hyperglycemia and dyslipidemia can lead to apoptosis [41]. In vitro, the autophagy and apoptosis of Schwann cells increase in hyperglycemia. According to our results, hyperglycemia decreases the expression of Lipin1 in the peripheral nerves, which further leads a disorder of lipid metabolism and then enhances cell autophagy. Excessive autophagy can increase apoptosis and aggravate diabetic neuropathy.

In the current study of autophagy in diabetic peripheral neuropathy, the researchers have reached different conclusions [35, 42, 43]. In in vivo and in vitro experiments, Qu Ling and Du W. et al. observed that in hyperglycemia, autophagy has been decreased, and Schwann cell damage is aggravated. However, Towns R. reported that autophagy in the spinal dorsal root neurons of STZ-induced diabetic

mice has been increased significantly, and neurons activate excessive autophagy, which may lead to neuronal loss and neuropathic pain. In our study, a similar result to Towns R. was observed, that is, hyperglycemia increases autophagy in sciatic nerve and Schwann cells, aggravating the damage of Schwann cells and sciatic nerves. Since autophagy is a continuous dynamic process, including autophagy formation and autophagy degradation, known as autophagy flow, different intervention times and intensities may affect the conclusion. It is necessary to further clarify whether the autophagy disorder is caused by increased autophagy formation or decreased degradation. Whether hyperglycemia increases or decreases autophagy in peripheral nerve tissue will also needs further studies. However, in the final analysis, hyperglycemia leads to the disorder of normal autophagy, resulting in the increased apoptosis of Schwann cells and aggravated DPN.

In summary, we demonstrated that Lipin1 plays an important role in the neuropathy of DPN rats. The loss of Lipin1 decreases DAG, which leads to lipid metabolism disorders. This condition increases autophagy and promotes DPN. Increased Lipin1 expression can reduce autophagy disorders and alleviate DPN. Hence, Lipin1 may be a potential target for DPN treatment via improved autophagy disorder in the future.

5. Conclusions

Hyperglycemia reduces the expression of Lipin1, prevents DAG synthesis, and activates autophagy, leading to increased apoptosis of Schwann cells. These factors cause demyelination and induce DPN. Lipin1 overexpression can alleviate autophagy disorders and improve DPN.

Abbreviations

7-AAD: 7-Aminoactinomycin D

ADV: Adenovirus

ADVs: Adenoviral vectors

BCA: Bicinchoninic acid

CCK-8: Cell Counting Kit-8

DAG: Diacylglycerol

DAPI: 4',6-diamidine-2-phenylidole dihydrochloride

DM: Diabetes mellitus

DMEM: Dulbecco’s modified Eagle’s medium

DPN: Diabetic peripheral neuropathy

ELISA: Enzyme linked immunosorbent assay

EM: Electron microscopy

FBS: Fetal bovine serum

FBG: Fasting-blood-glucose

FITC: Fluorescein isothiocyanate

LV: Lentivirus

LVs: Lentiviral vectors

MNCV: Motor nerve conduction velocity

MOI: Multiplicity of infection

NC: Negative control

PA: Phosphatidic acid

PAP: Phosphatidic acid phosphatase

PBS: Phosphate buffered saline

PKD: Protein kinase D

PMWT: Paw mechanical withdrawal threshold

PVDF: Polyvinylidene fluoride

qPCR: Quantitative real-time polymerase chain reaction

SDS-PAGE: Sodium dodecyl sulfate polyacrylamide gel electrophoresis

STZ: Streptozotocin

TBS-T: Tris Buffered saline Tween

Author Declarations

Consent for Publication All authors agree to publish the article in this magazine and the manuscript contains no any individual person's data in any form.

Availability of Data and Material All data generated or analysed during this study are included in this published article and are available from the corresponding author upon reasonable request.

Competing Interests The authors report that they have no competing interests.

Funding This study was supported by the National Natural Science Foundation of China (NNSFC) (NO.81670753 and NO. 82070847) to S.C., and NNSFC (NO.81800722) to X.Z., the grants from the Key R & D programs of Shandong Province (No.2018GSF118108) to S.C., and the Hospital Youth Foundation of Qilu Hospital of Shandong University, Qingdao (QDKY2017QN12) to M.W.

Authors' Contributions S.C. conceived the study. X.Z., S.Y., L.C. and S.C. designed the study. M.W., M.X., P.S, C.Z., X.H. and C.F. performed the experiments and interpreted data analyses. M.W. wrote the first version of the paper. All authors critically reviewed, revised, and approved the final version of the manuscript.

Acknowledgments Thanks for the guidance of the teachers from the Institute of basic medicine of Shandong University and the provision of the rat sciatic nerve conduction velocity meter. We also thank the teachers of the basic laboratory of the Second Hospital of Shandong University for their guidance in the research of apoptosis.

Compliance with Ethical Standards

Ethics approval and consent to participate This article does not contain any studies with human participants performed by any of the authors. Animal experiments were performed in accordance with the International Guiding Principles for Animal Research as stipulated by the World Health Organization were followed.

Conflicts of interest The authors declare that they have no conflict of interest.

ORCID Meijian Wang: 0000-0003-1021-2421

Shihong Chen: 0000-0002-5488-2139

References

1. Saeedi P, Petersohn I, Salpea P, Malanda B, Karuranga S, Unwin N, Colagiuri S, Guariguata L, Motala AA, Ogurtsova K, Shaw JE, Bright D, Williams R; IDF Diabetes Atlas Committee. Global and regional diabetes prevalence estimates for 2019 and projections for 2030 and 2045: Results from the International Diabetes Federation Diabetes Atlas, 9th edition. Diabetes Res Clin Pract. 2019 Nov;157:107843
2. International Diabetes Federation (2017) IDF Diabetes Atlas, 8th edn. International Diabetes Federation, Brussels
3. Chatterjee S, Khunti K, Davies MJ (2017) Type 2 diabetes. Lancet 389(10085):2239–2251
4. Lin S, Rocha VM, Taylor R (2019) Artefactual inflation of type 2 diabetes prevalence in WHO STEP surveys. Trop Med Int Health TM IH 24(4):477–483

5. Tesfaye S, Selvarajah D, Gandhi R et al. Diabetic peripheral neuropathy may not be as its name suggests: evidence from magnetic resonance imaging. Pain. 2016 Feb; 157 Suppl 1: S72-S80
6. Alleman CJ, Westerhout KY, Hensen M, Chambers C, Stoker M, Long S, van Nooten FE (2015) Humanistic and economic burden of painful diabetic peripheral neuropathy in Europe: A review of the literature. Diabetes Res Clin Pract 109(2):215–225
7. Sloan G, Shillo P, Selvarajah D, Wu J, Wilkinson ID, Tracey I, Anand P, Tesfaye S (2018 Oct) A new look at painful diabetic neuropathy. Diabetes Res Clin Pract 144:177–191
8. Tesfaye S, Boulton AJ, Dickenson AH (2013) Mechanisms and management of diabetic painful distal symmetrical polyneuropathy. Diabetes Care 36(9):2456–2465
9. Feldman EL, Nave KA, Jensen TS, Bennett DL (2017) New Horizons in Diabetic Neuropathy: Mechanisms, Bioenergetics, and Pain. Neuron 93(6):1296–1313
10. Ghavami S, Shojaei S, Yeganeh B et al (2014 Jan) Autophagy and apoptosis dysfunction in neurodegenerative disorders. Prog Neurobiol 112:24–49
11. Mijaljica D, Prescott M, Devenish RJ (2011 Jul) Microautophagy in mammalian cells: revisiting a 40-year-old conundrum. Autophagy 7(7):673–682
12. Maycotte P, Guemez-Gamboa A, Moran J. Apoptosis and autophagy in rat cerebellar granule neuron death: Role of reactive oxygen species. J Neurosci Res. 2010 Jan; 88(1):73–85
13. Wang QJ, Ding Y, Kohtz DS et al. Induction of autophagy in axonal dystrophy and degeneration. J Neurosci. 2006 Aug 2; 26(31):8057–68
14. Tang SQ, Jiang QY, Yang CF et al (2010 Oct) Research and development of Lipin family. Yi Chuan 32(10):981–993
15. Mul JD, Nadra K, Jagalur NB et al. A hypomorphic mutation in Lpin1 induces progressively improving neuropathy and lipodystrophy in the rat. J Biol Chem. 2011 Jul 29; 286(30):26781–93
16. Pan S, Fengjie Z, Feng H et al. Lipin1 mediates cognitive impairment in fld mice via PKD-ERK pathway. Biochem Biophys Res Commun. 2020 Apr 30;525(2):286–291
17. Min X, Meijian W, Wei L et al (2020 Oct) Lipin1 is involved in the pathogenesis of diabetic encephalopathy through the PKD/Limk/Cofilin signaling pathway. Oxid Med Cell Longev 16:2020:1723423
18. Xu Wang C, Wang J, Zeng et al (2005 Aug) Gene Transfer to Dorsal Root Ganglia by Intrathecal Injection: Effects on Regeneration of Peripheral Nerves. Mol Ther 12(2):314–320
19. Njoo C, Heinl C, Kuner R (2014 Mar) In vivo SiRNA transfection and gene knockdown in spinal cord via rapid noninvasive lumbar intrathecal injections in mice. J Vis Exp 22;(85):51229
20. Taliyan R, Sharma PL (2012) Possible mechanism of protective effect of thalidomide in STZ-induced-neuropathic pain behavior in rats. Inflammopharmacology 20(2):89–97
21. Kishore L, Kaur N, Singh R (2018 Aug) Effect of Kaempferol isolated from seeds of Eruca sativa on changes of pain sensitivity in Streptozotocin-induced diabetic neuropathy. Inflammopharmacology 26(4):993–1003

22. Livak KJ, Schmittgen TD (2001 Dec) Analysis of relative gene expression data using real-time quantitative PCR and the $2^{-\Delta\Delta Ct}$ method. Methods 25(4):402–408
23. Xianghua Zhuang X, Li G, Qian et al (2015) Changes of Lipin1β Expression in Gestational Diabetes Mellitus. Clinical Laboratory 61(3–4):307–313
24. Cameron NE, Eaton SE, Cotter MA, Tesfaye S (2001) Vascular factors and metabolic interactions in the pathogenesis of diabetic neuropathy. Diabetologia 44(11):1973–1988
25. Tesfaye S, Harris ND, Wilson RM, Ward JD (1992) Exercise-induced conduction velocity increment: a marker of impaired peripheral nerve blood flow in diabetic neuropathy. Diabetologia 35(2):155–159
26. Oates PJ (2002) Polyol pathway and diabetic peripheral neuropathy. Int Rev Neurobiol 50:325–392
27. Wada R, Yagihashi S (2005) Role of advanced glycation end products and their receptors in development of diabetic neuropathy. Ann N Y Acad Sci 1043:598–604
28. Anand P, Terenghi G, Warner G, Kopelman P, Williams-Chestnut RE, Sinicropi DV (1996) The role of endogenous nerve growth factor in human diabetic neuropathy. Nat Med 2(6):703–707
29. Callaghan BC, Cheng HT, Stables CL, Smith AL, Feldman EL (2012) Diabetic neuropathy: clinical manifestations and current treatments. Lancet Neurol 11(6):521–534
30. Stavoe AKH, Holzbaur ELF. Autophagy in Neurons. Annu Rev Cell Dev Biol. 2019 Oct 6;35:477–500
31. Scrivo A, Codogno P, Bomont P. Gigaxonin E3 ligase governs ATG16L1 turnover to control autophagosome production. Nat Commun. 2019 Feb 15;10(1):780
32. Donkor J, Sariahmetoglu M, Dewald J, Brindley DN, Reue K (2007) Three mammalian lipins act as phosphatidate phosphatases with distinct tissue expression patterns. J Biol Chem 282:3450–3457
33. Han GS, Wu WI, Carman GM (2006) The Saccharomyces cerevisiae Lipin homolog is a Mg^{2+}-dependent phosphatidate phosphatase enzyme. J Biol Chem 281:9210–9218
34. Zhang P, Verity MA, Reue K. Lipin-1 Regulates Autophagy Clearance and Intersects with Statin Drug Effects in Skeletal Muscle. Cell Metab. 2014 August 5; 20(2): 267–279
35. Qu L, Zhang H, Gu B et al (2016 Mar) Jinmaitong Alleviates the diabetic peripheral neuropathy by inducing autophagy. Chin J Integr Med 22(3):185–192
36. Liu Y, Chen X, Yao J et al (2019) Circular RNA ACR relieves high glucose-aroused RSC96 cell apoptosis and autophagy via declining microRNA-145-3p. J Cell Biochem. Dec 30
37. Wang X, Huan Y, Li C et al (2020 Sep) Diphenyl diselenide alleviates diabetic peripheral neuropathy in rats with streptozotocin-induced diabetes by modulating oxidative stress. Biochem Pharmacol 16:182:114221
38. Muscella A, Vetrugno C, Cossa LG et al (2020 May) TGF-β1 activates RSC96 Schwann cells migration and invasion through MMP-2 and MMP-9 activities. J Neurochem 153(4):525–538
39. Mir SU, Schwarze SR, Jin L et al (2013 Oct) Progesterone receptor membrane component 1/Sigma-2 receptor associates with MAP1LC3B and promotes autophagy. Autophagy 9(10):1566–1578
40. Del Bello B, Marcolongo P, Ciarmela P et al (2019 Dec) Autophagy up-regulation by ulipristal acetate as a novel target mechanism in the treatment of uterine leiomyoma: an in vitro study. Fertil Steril

112(6):1150–1159

41. Gomez-Sanchez JA, Carty L, Iruarrizaga-Lejarreta M et al. Schwann cell autophagy, myelinophagy, initiates myelin clearance from injured nerves. J Cell Biol. 2015 Jul 6; 210(1):153–68
42. Towns R, Guo C, Shangguan Y et al. Type 2 diabetes with neuropathy: autoantibody stimulation of autophagy via Fas. Neuroreport. 2008 Feb 12; 19 (3):265–9
43. Du W, Wang N, Li F et al (2019 Jul) STAT3 phosphorylation mediates high glucose-impaired cell autophagy in an HDAC1-dependent and -independent manner in Schwann cells of diabetic peripheral neuropathy. FASEB J 33(7):8008–8021

Figures

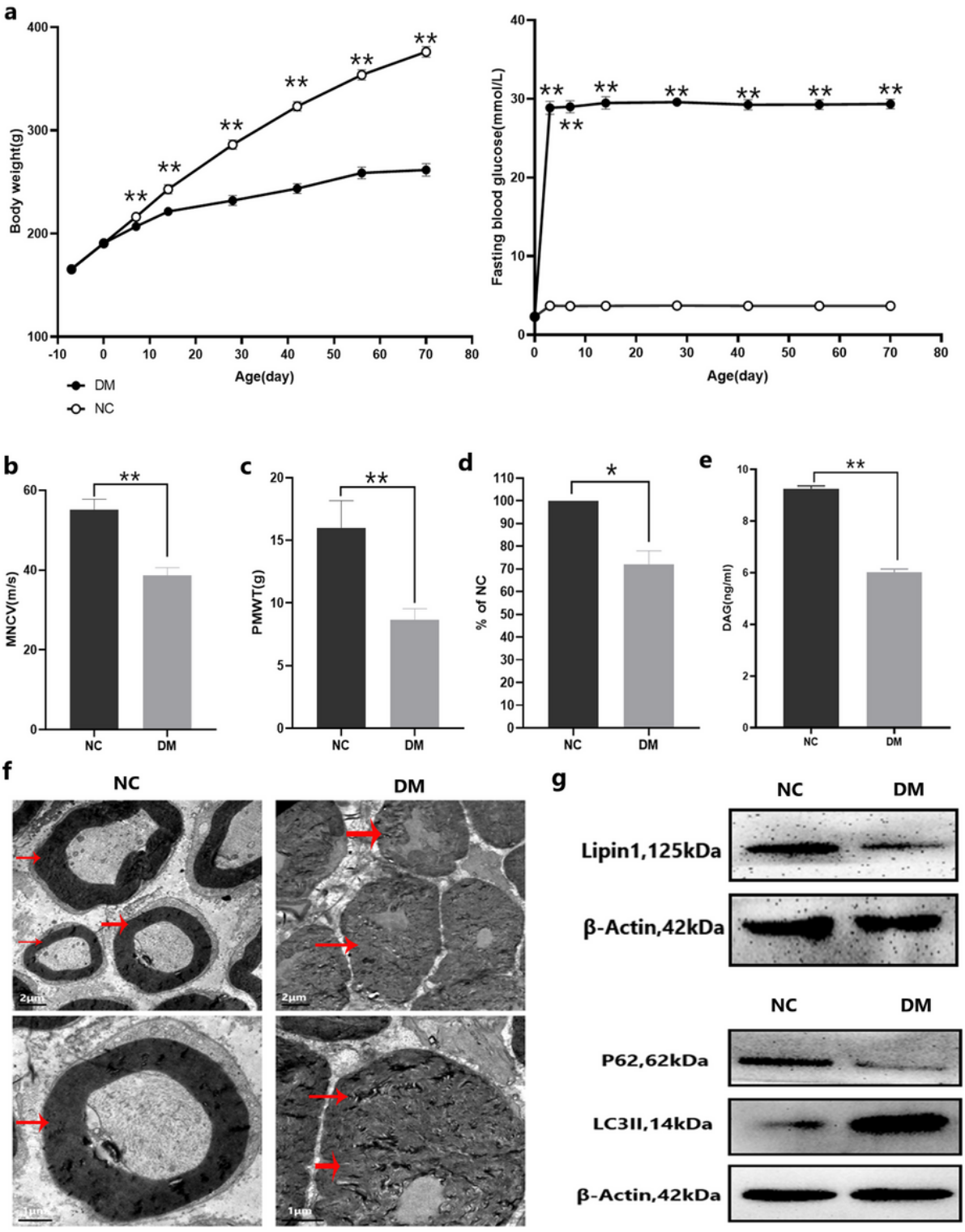

Figure 1

Decreased Lipin1 and demyelination of sciatic nerve inDPN rats. (a) Changes in body weights and blood glucose levels in rats after STZ injection (n=6 animals/group). (b) Changes of the motor nerve conductive velocity (MNCV) between diabetic rats (DM) vs negative control rats (NC) (n=6 animals/group). (c) Changes of the paw mechanical withdrawal threshold (PMWT) between DM and NC group (n=6 animals/group). (d) Lipin1 mRNA expression as determined using qPCR between DM and NC group (n=3

animals/group). (e) The levels of diacylglycerol (DAG) between DM and NC group (n=3 animals/group). (f) Demyelination of sciatic nerve in DM rats occur, the lamella is loose and broken (scale bar = 2 μm and 1 μm). Arrows indicate the lamella. (g) Lipin1, LC3II and P62 protein expressions as determined using Western blot (n=3 animals/group). Data are presented as the means ± SEMs. *P < 0.05, **P < 0.01 versus NC group.

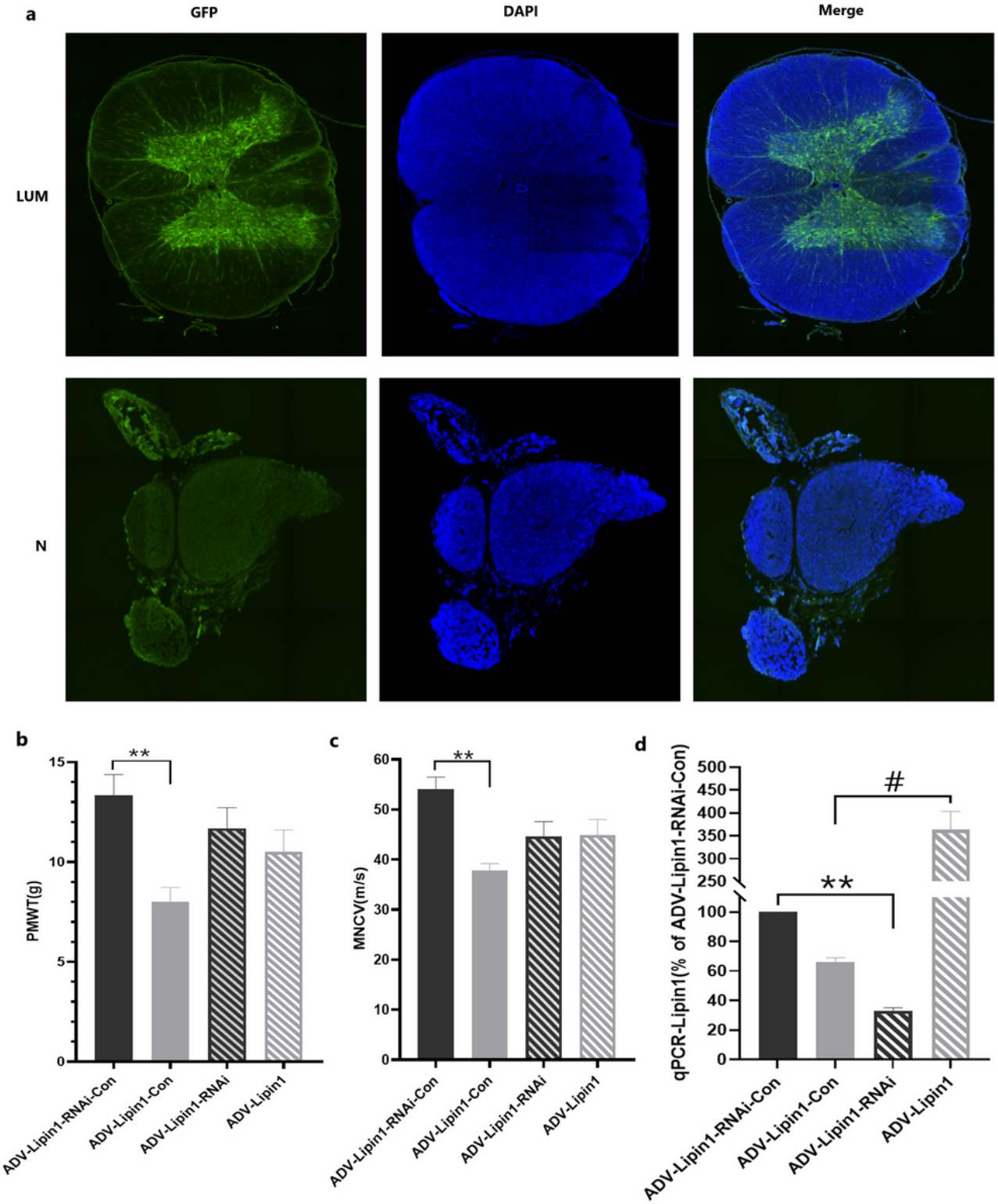

Figure 2

Lipin1 regulated function of sciatic nerve in DPN and NC rats. (a) Illustration of viral infusion of ADV into the lumbar spinal cord and sciatic nerve (scale bar = 200 μm). (b) Changes of MNCV after different ADVs injection between ADV-Lipin1-RNAi-Con, ADV-Lipin1-Con, ADV-Lipin1-RNAi and ADV-Lipin1 group (n=6 animals/group). (c) Changes of PMWT after different ADVs injection between ADV-Lipin1-RNAi-Con, ADV-Lipin1-Con, ADV-Lipin1-RNAi and ADV-Lipin1 group (n=6 animals/group). (d) Lipin1 mRNA expression as determined using qPCR after different ADVs injection between ADV-Lipin1-RNAi-Con, ADV-Lipin1-Con, ADV-Lipin1-RNAi and ADV-Lipin1 group (n=3 animals/group). Data are presented as the means ± SEMs. **P < 0.01 versus ADV-Lipin1-RNAi-Con group; #P < 0.05 versus ADV-Lipin1- Con group.

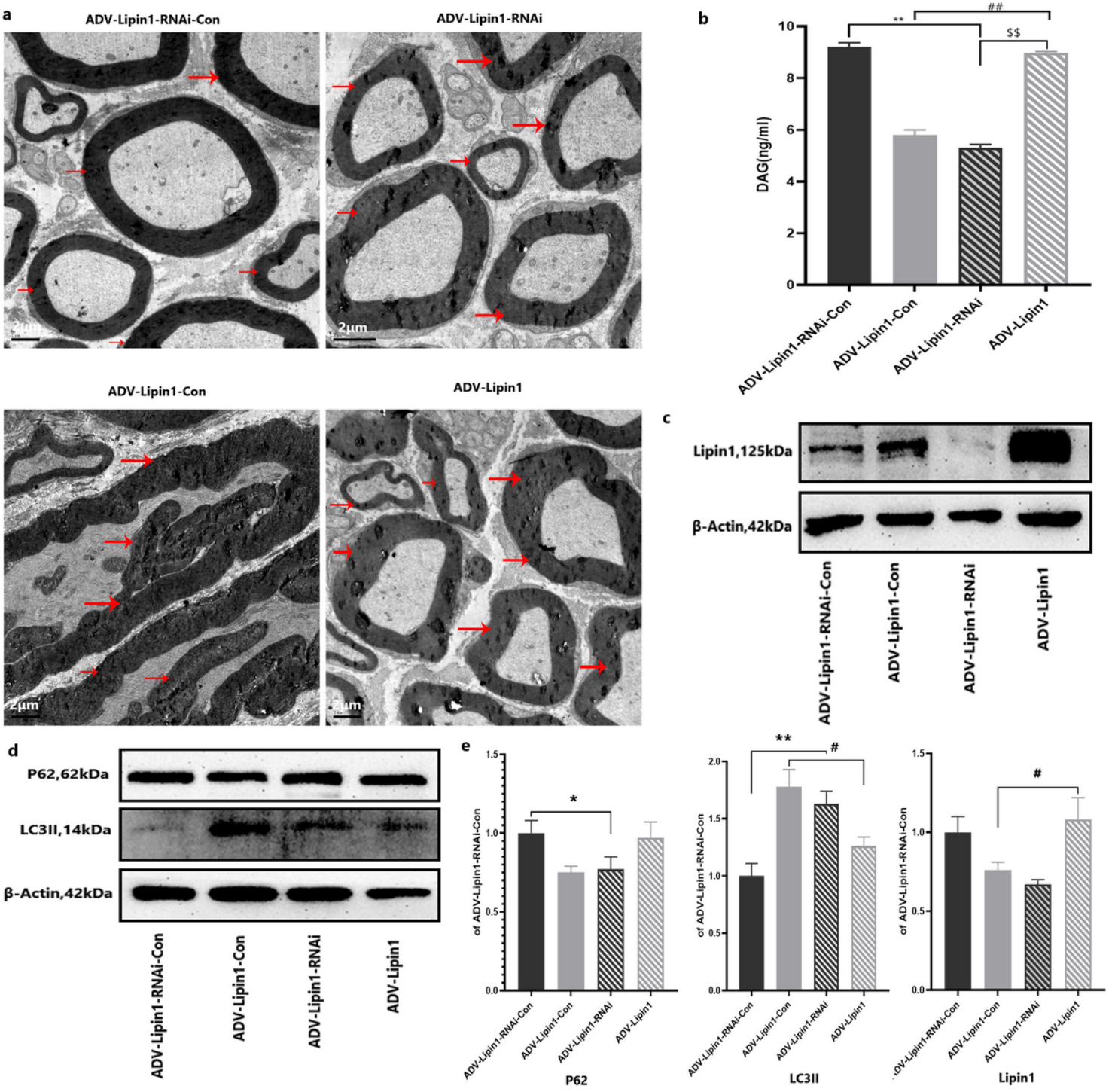

Figure 3

Lipin1 regulated morphological changes and autophagy in DPN and NC rats. (a) Morphological changes of sciatic nerve after intrathecal injection of different ADVs in DPN and NC rats. (scale bar = 2 μm). Arrows indicate the lamella. (b) Changes of DAG after different ADVs injection between ADV-Lipin1-RNAi-Con, ADV-Lipin1-Con, ADV-Lipin1-RNAi and ADV-Lipin1 group (n=3 animals/group). (c) Lipin1 protein expressions as determined using Western blot after different ADVs injection between ADV-Lipin1-RNAi-Con, ADV-Lipin1-Con, ADV-Lipin1-RNAi and ADV-Lipin1 group (n=3 animals/group). (d) LC3II and P62 protein expressions as determined using Western blot after different ADVs injection between ADV-Lipin1-RNAi-Con, ADV-Lipin1-Con, ADV-Lipin1-RNAi and ADV-Lipin1 group (n=3 animals/group). (e) Lipin1, LC3II and P62 protein expressions as determined using Western blot after different ADVs injection between ADV-Lipin1-RNAi-Con, ADV-Lipin1-Con, ADV-Lipin1-RNAi and ADV-Lipin1 group (n=3 animals/group). Data are presented as the means ± SEMs. *P < 0.05, **P < 0.01 versus ADV-Lipin1-RNAi-Con group; #P < 0.05, ##P < 0.01 versus ADV-Lipin1- Con group; $$P < 0.01 versus ADV-Lipin1-RNAi group.

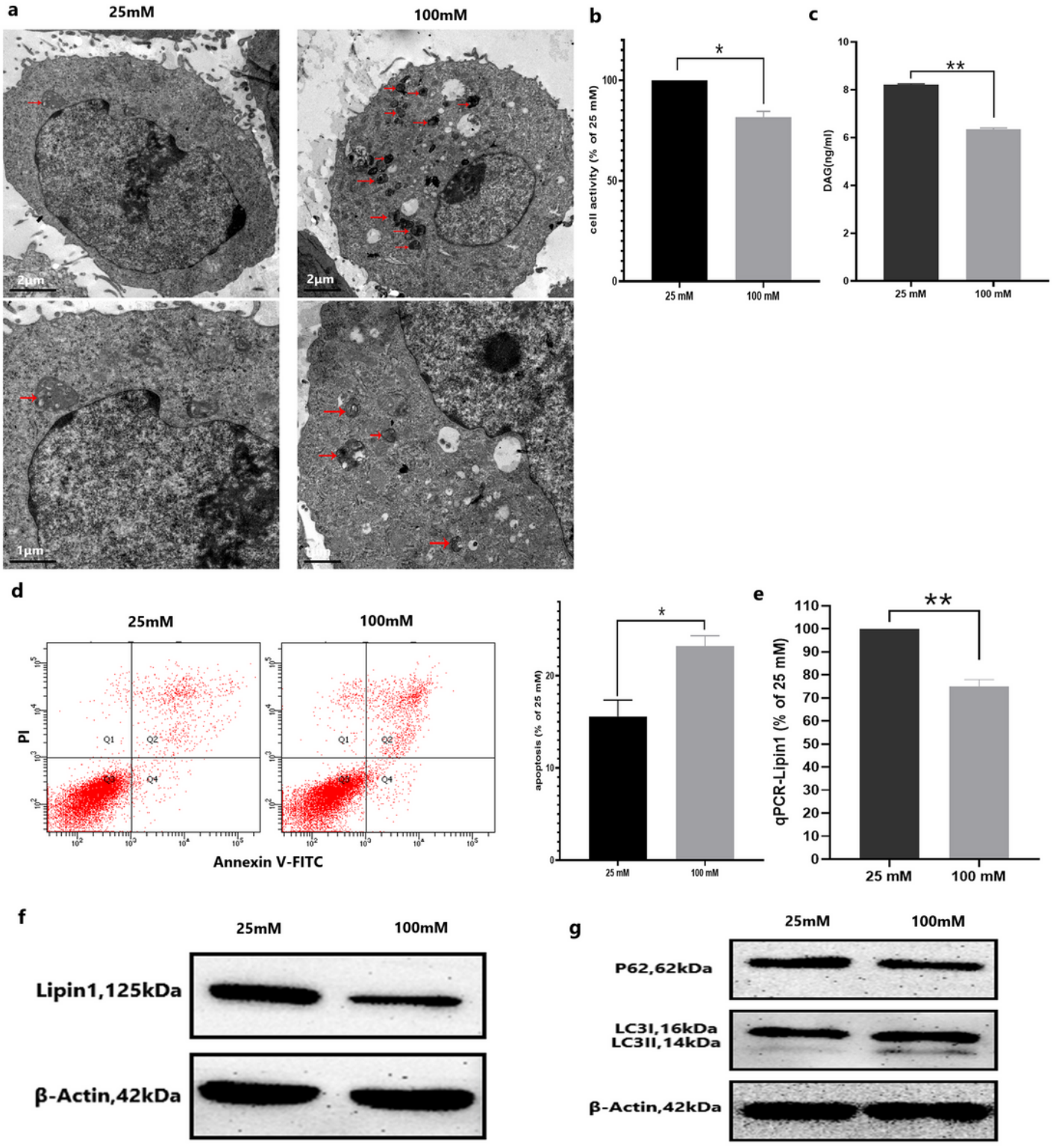

Figure 4

Changes in RSC96 cell viability in response to high glucose toxicity are related to Lipin1. (a) High glucose-induced autophagic bodies observed using electron microscope (scale bar = 2 μm and 1 μm). Arrows indicate the autophagic bodies. (b) Cell activity after 48h of treatment with normal glucose (25mM) versus high glucose (100mM). (c) DAG levels between 25mM and 100mM. (d) FACS apoptosis assay results using FITC-Annexin V and PI staining at 48h. (e) Lipin1 mRNA expression as determined using

qPCR between 25mM and 100mM. (f) Lipin1 protein expressions as determined using Western blot between 25mM and 100mM. (g) LC3II and P62 protein expressions as determined using Western blot between 25mM and 100mM. Data are presented as the means ± SEMs. *P < 0.05, **P < 0.01 versus 25mM.

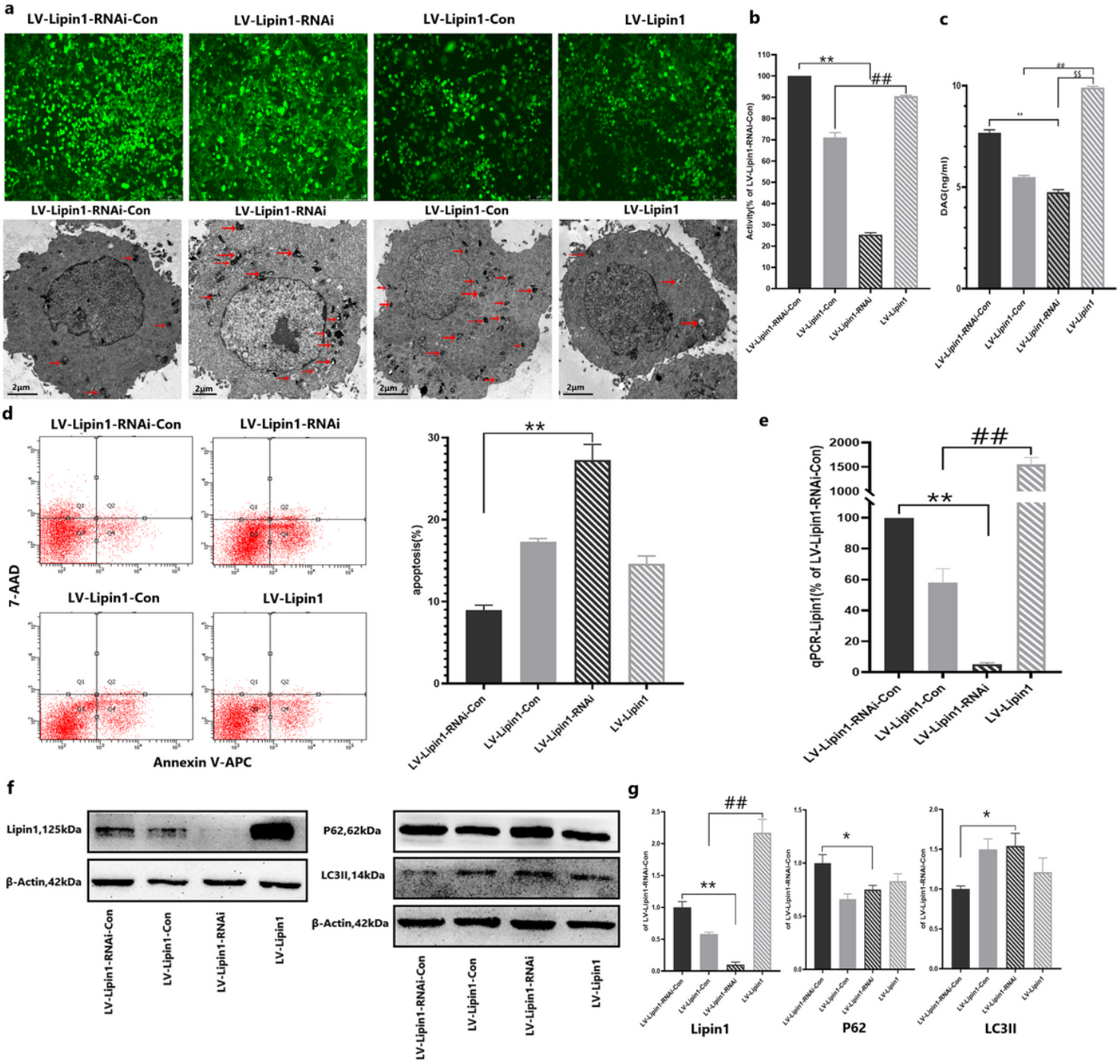

Figure 5

Lipin1 regulated autophagy in RSC96 cells. (a) Illustration of viral infusion of LVs in RSC96 cells (scale bar = 25 μm and 75 μm) and autophagic bodies observed using electron microscope (scale bar = 2 μm). Arrows indicate the autophagic bodies. (b) Cell activity after different LVs transfected between LV-Lipin1-RNAi-Con, LV-Lipin1-Con, LV-Lipin1-RNAi and LV-Lipin1 group. (c) DAG levels after different LVs

transfected between LV-Lipin1-RNAi-Con, LV-Lipin1-Con, LV-Lipin1-RNAi and LV-Lipin1 group. (d) ACS apoptosis assay results using APC-Annexin V and 7-AAD staining at 48h after LVs infection. (e) Lipin1 mRNA expression as determined using qPCR after different LVs injection between LV-Lipin1-RNAi-Con, LV-Lipin1-Con, LV-Lipin1-RNAi and LV-Lipin1 group. (f, g) Lipin1, LC3II and P62 protein expressions as determined using Western blot after different LVs injection between LV-Lipin1-RNAi-Con, LV-Lipin1-Con, LV-Lipin1-RNAi and LV-Lipin1 group. Data are presented as the means ± SEMs. *P < 0.05, **P < 0.01 versus LV-Lipin1-RNAi-Con group; ##P < 0.01 versus LV-Lipin1- Con group; $$P < 0.01 versus LV-Lipin1-RNAi group.